Earthquakes and Structures, *Vol. 6, No. 5 (2014) 561-580*
DOI: http://dx.doi.org/10.12989/eas.2014.6.5.561

Seismic behavior of frames with innovative energy dissipation systems (FUSEIS 1-1)

Georgia Dougka*, Danai Dimakogianni[a] and Ioannis Vayas[b]

School of Civil Engineering, National Technical University of Athens,
Iroon Polytechniou 9, 15772 Zografou, Greece

(Received July 8, 2013, Revised January 5, 2014, Accepted January 14, 2014)

Abstract. After strong earthquakes conventional frames used worldwide in multi - story steel buildings (e.g. moment resisting frames) are not well positioned according to reparability. Two innovative systems for seismic resistant steel frames incorporated with dissipative fuses were developed within the European Research Program "FUSEIS" (Vayas *et al.* 2013). The first, FUSEIS1, resembles a vertical Vierendeel beam and is composed of two closely spaced strong columns rigidly connected to multiple beams. In the second system, FUSEIS2, a discontinuity is introduced in the composite beams of a moment resisting frame and the dissipative devices are steel plates connecting the two parts. The FUSEIS system is able to dissipate energy by means of inelastic deformations in the fuses and combines ductility and architectural transparency with stiffness. In case of strong earthquakes damage concentrates only in the fuses which behave as self-centering systems able to return the structure to its initial undeformed shape. Repair work after such an event is limited only to replacing the fuses. Experimental and numerical investigations were performed to study the response of the fuses system. Code relevant design rules for the seismic design of frames with dissipative FUSEIS and practical recommendations on the selection of the appropriate fuses as a function of the most important parameters and member verifications have been formulated and are included in a Design Guide. This article presents the design and performance of building frames with FUSEIS 1-1 based on models calibrated on the experimental results.

Keywords: innovative; seismic; systems; fuses; beams

1. Introduction

Conventional earthquake engineering has been focused on the protection of human life. The design of traditional seismic resisting systems uses energy dissipation mechanisms in selected structural parts (members or connections) to protect the building against collapse. However, when plastic hinges are formed in structural members they may lead to excessive permanent drifts due to inelastic deformations. As a consequence, after a major seismic event building demolition may seem more reasonable compared to high repair costs.

During the last years the attention of research has been concentrated on the development of systems able to restrict plastic deformations in "repairable" fuses which not only prevent collapse but also limit structural damage and allow for immediate occupancy after earthquake. Several

*Corresponding author, Ph.D. Student , E-mail: yiouli@dougka.gr
[a]Ph.D. Student , E-mail: d_dimakogianni@hotmail.com
[b]Professor, E-mail: vastahl@central.ntua.gr

http://www.techno-press.org/?journal=eas&subpage=7 ISSN: 2092-7614 (Print), 2092-7622 (Online)

systems with efficient seismic performance have been introduced such as the dissipative connections used in seismic resistant braced steel frames (INERD) (Plumier *et al.* 2004; Vayas *et al.* 2005; Vayas *et al.* 2006;Vayas *et al.* 2007), Post-Tensioned Energy Dissipating (PTED) steel frame (Christopoulos *et al.* 2002), buckling-restrained braces (BRBs) (Saeki *et al.* 1996; Sabelli et *al.* 2003), added damping and stiffness devices (ADAS) and triangular added damping and stiffness devices (TADAS) (Tsai *et al.* 1993; Dargush and Soong, 1995; Tena-Colunga 1997), and steel shear panel devices (Nakashima 1995; Nakashima *et al.*, 1995).

Similarly, the FUSEIS system limits the plasticization within the system devices while the system columns and the gravity frame are protected and undamaged. As the intensity of the earthquake increases the structure passes from the elastic state to the formation of plastic hinges only in the fuses which are repairable and replaceable while the gravity system remains elastic. Additionally to its good seismic performance the FUSEIS system may consist an economically competitive solution against other systems since the fuses are small with a simple detail and calculation procedure which facilitate their fabrication and make them accessible to the construction industry.

2. Description of FUSEIS 1

This innovative system is composed of two closely spaced strong columns rigidly connected to multiple beams, having the additional advantages of energy dissipation through plastic deformation of the beams and ease of repair and even replacement if necessary. The beams run from column to column, FUSEIS 1-1, or alternatively are interrupted and connected by short pins, FUSEIS 1-2, (Dimakogianni *et al*. 2012). This study presents the results of the seismic performance of frames with FUSEIS1-1.

The system resists lateral loads similar to a vertical Vierendeel beam, mainly by combined bending and shear of the beams and axial forces of the columns. The dissipative elements of the system are the FUSEIS beams which are not generally subjected to vertical loads as they are placed between floor levels.

The seismic resistance of a building may be obtained by appropriate incorporation of a number of such systems in the relevant directions (Fig. 1). When floor beam-to-column connections of the building are formed as simple, this system provides the entire seismic resistance of the building. When these connections are rigid or semi-rigid it works in combination with the overall moment resisting frame. The connection of the floor beams to the columns that compose the FUSEIS system should be preferably simple in order to avoid design of the FUSEIS columns by capacity design considerations in respect to the strong floor beams and introduce capacity design in respect to the weak FUSEIS beams only.

The fuses-to-column joints are formed as rigid to enable the Vierendeel action and are designed to have sufficient overstrength in order to achieve energy absorption only in the fuses. Bolted end-plate connections which enable an easy replacement of the beams are used. Considering a typical floor height of 3.4 m, four or five beams may be placed per story. The beam height depends on the required stiffness with the provision to leave the necessary vertical spacing between them. In addition, one fuse is provided between columns just above foundation level to minimize the moment transfer to the foundation and enable the realization of simple/pinned bases for FUSEIS columns.

FUSEIS columns may be of open or closed section. Open sections are more beneficial for constructional purposes, since they offer easier connection to the beams. When closed sections are

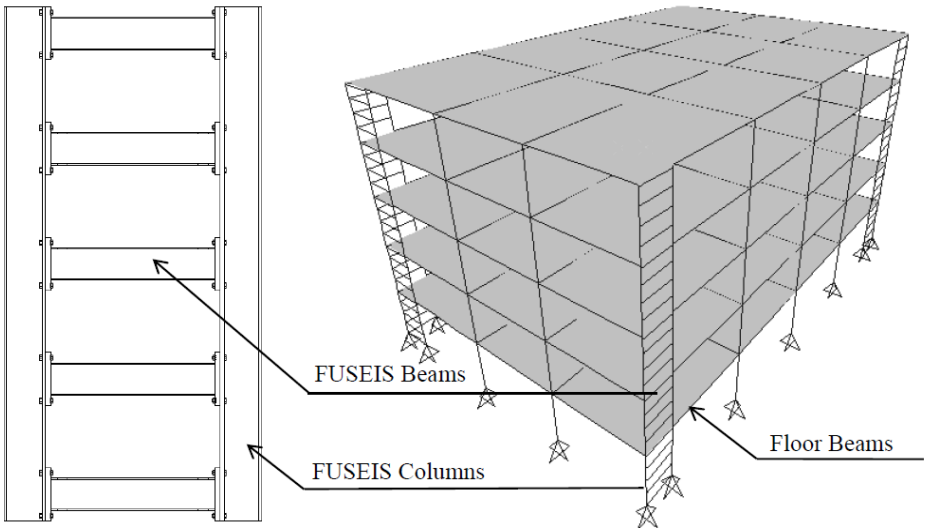

Fig. 1 Incorporation of FUSEIS 1 systems in a building

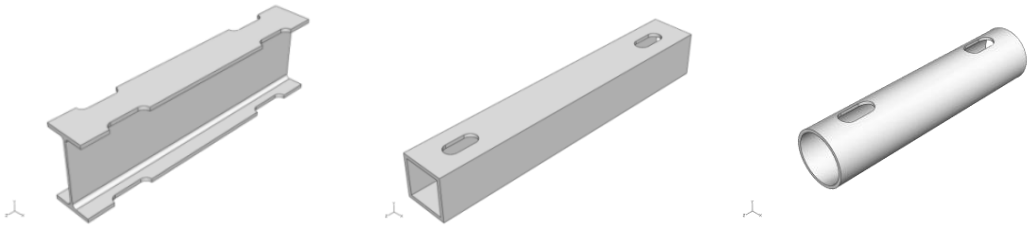

Fig. 2 FUSEIS 1-1 beams (RBS sections at beam ends)

Table 1 Geometry of RBS

$a = 50\ mm - 0{,}50 * b_f$	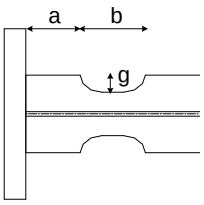	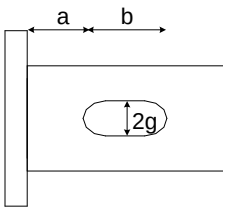
$b = 75\ mm - 0{,}65 * d_b$		
$g \leq 0{,}25 * bf$		

used, as appropriate at building corners with FUSEIS beams in both directions,T-sections can be welded to offer the advantage of easier connection.

FUSEIS beams may have hollow sections (RHS or CHS) or open sections (I or H). Hollow sections are more beneficial to open sections due to their larger flexural and torsional rigidities.

To achieve a sequential plasticization of the fuses, beam sizes may vary between floors following the increase of story shear from the top to the base of the building. In addition, beams may also vary within the floor either in respect to their size or to their length.

In order to lead the plastic hinge to form away from the connection area and protect the beam to column connections of the system against fracture, beam flanges are reduced near the ends CEN (2

004) EC3 (Fig. 2). Constant, tapered or radius cut shapes may be used to reduce the cross sectional area. Table 1 gives recommendations for the dimensions of the RBS members.

As an alternative, the connection region could be strengthened by additional plates/stiffeners.

Excessive overstrength of the dissipative elements is avoided by selecting the steel of these beams in accordance with the CEN (2003)EC 8 – rules to have a maximum value of yield strength

$$f_{y,\max} \leq 1{,}1 \cdot \gamma_{ov} \cdot f_y \tag{1}$$

where

γ_{ov} =1,25

f_y = nominal value of the yield strength

It is advisable to use S 235 steel for the beams. In this instance, Eq. (1) yields $f_{y,max}$ = 323 MPa. The value of $f_{y,max}$ shall be referred to in the design drawings.

3. Preliminary design

As previously mentioned the FUSEIS1 system works as a vertical Vierendeel beam. At the ultimate limit state all beams reach their moment capacity as they are the dissipative elements of the system. Therefore, the story shear that may be transferred when the FUSEIS beams are provided with RBS-sections at distance l_{RBS} is equal to

$$V_{storey} = \frac{2 \cdot \sum M_{pl,RBS,Rd}}{h_{storey}} \frac{L}{l_{RBS}} \tag{2}$$

where

$M_{pl,RBS,Rd} = W_{pl,RBS} \cdot f_y$ = design moment resistance of RBS FUSEIS beam section

l_{RBS} = axial distance between RBS sections

L = axial distance of FUSEIS columns

If the total base shear of the building is V_B the number of systems to be used for a preliminary design is equal to

$$m = \frac{V_B}{V_{storey}} \tag{3}$$

The column sections are chosen primarily from stiffness considerations and were defined by limitations of interstory drifts and 2nd order effects. In addition, for m equal FUSEIS systems the FUSEIS columns have to resist at least an axial force

$$N_{c,Ed} = \frac{M_{ov}}{m \cdot L} \tag{4}$$

where

M_{ov} = overturning moment of the frame

The cross sections for beams and columns of the system as well as the required number of systems cannot be estimated from strength criteria alone. The deformations shall be also controlled in order to limit 2nd order effects according to the relevant provisions.

At global inter-story drift rotations θ_{gl} of the frame during seismic loading the dissipative elements, beams, exhibit larger plastic rotations calculated from

$$\theta_{pl,RBS} = \frac{L}{l_{RBS}}\theta_{gl} \quad (5)$$

where,

$\theta_{pl,RBS}$ = plastic rotation of the fuse beam

L = axial distance of columns

l_{RBS}= axial distance between plastic hinges – net length of beams

4. Design of frames

Based on the understanding gained from the full scale tests on frames with FUSEIS 1-1 performed in the National Technical University of Athens 2D building frames with fuses were designed and analyzed using the general purpose software Code SAP 2000. In addition to conventional design, non-linear static and dynamic analyses were carried out to estimate the behavior factor of the system. Non-linear analyses were based on the response of the devices which have been experimentally investigated.

Several building frames with fuses were designed according to the provisions of EC3 and EC8 (CEN (2003)). Additional rules given in the relevant Design Guide (Vayas *et al.*, 2012) were applied to ensure that yielding, takes place in the FUSEIS beams prior to any yielding or failure elsewhere. The FUSEIS beams, able to dissipate energy by the formation of plastic bending mechanisms, were designed to resist the forces of the most unfavourable seismic combination.

Since this system module is used to ensure lateral stiffness and seismic energy dissipation for building structures, the frames were dimensioned to cover the Seismic zones corresponding to the Greek earthquake intensity conditions 0,16g, 0,24g, 0,36g. In order to reflect the findings obtained during the experimental program the cross sections used were similar to the ones tested (IPE, SHS, CHS). All fuses beam sections were reduced near the ends by approximately 30%. For each type of fuse section a 2D frame was examined for the three seismic accelerations resulting in total nine 2D frames. These models provided an optimal approximation of the behavior of a steel building.

A typical 2D building frame, part of a five-story composite building, was used for all the cases examined (Fig. 3). The composite building consisted of similar frames at 8m axial distance which was the effective width for both the vertical loads and the lateral mass during earthquake loading. The bays of the main frame were 6,0 m. The beams were composite and the thickness of the slab was 15cm. The effective width of the composite beams was equal to 1,5m in accordance with EC2.

The FUSEIS system consisted of two closely positioned vertical hollow strong columns, jointed together with five horizontal beams in a tight arrangement. The center line distance of the columns was 2m.

To simulate the hysteretic behavior of fuses rigid zones were provided from column centers to column faces to exclude non-existent beam flexibilities. The net length of beam fuses was subdivided to 5 zones that represent the full sections (ends – middle) and the RBS-sections. In this manner, the true system flexibility and strength were accounted for. The remaining structural elements were represented as usual.

Generally, pin connections were introduced at the column bases to prevent the damage of the columns and protect the foundation. In order to introduce partial fixity conditions between the

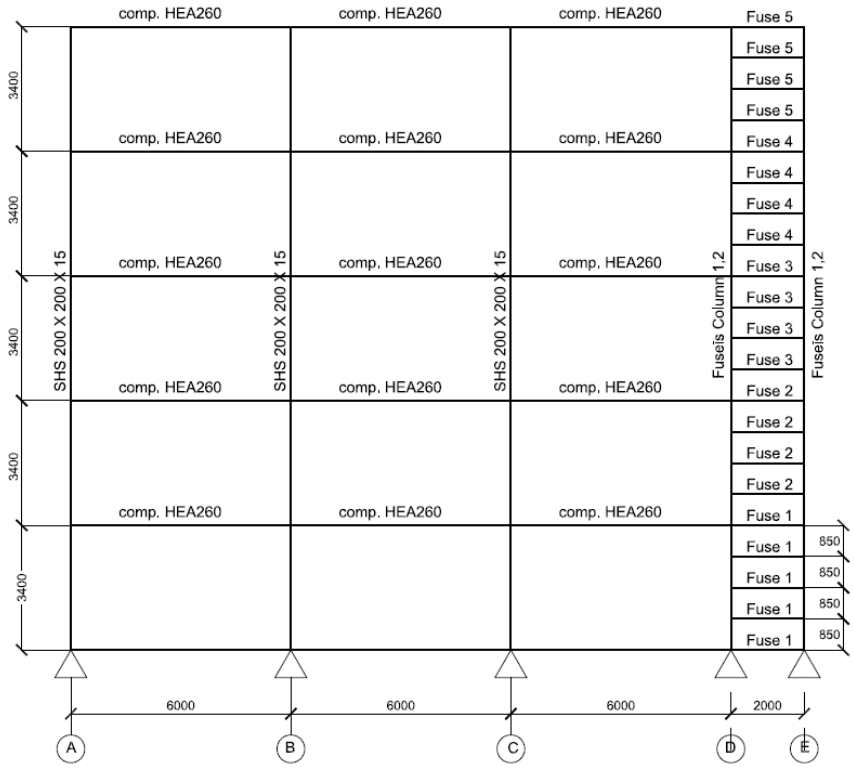

Fig. 3 Typical 2D building frame

Table 2 Assumptions for materials and loads

Materials	
Concrete	C25/30, γ = 25KN/m^3, E = 31GPa
Reinforcement	B500C
Structural steel	S235: Dissipative elements (FUSEIS) S355: Non dissipative elements (beams - columns)
Vertical loads	
Dead loads apart from self-weight – G	2,00kN/m^2
Live loads – Q	2,00kN/m^2
Seismic loads	
Elasticresponsespectra	Type 1
Peakgroundacceleration	A = 0,16g – 0,24g – 0,36g
Importance class	II
Groundtype	B
Behaviorfactor q	5,00
Damping	5%
Factors of operating loads for seismic combinations	φ = 1,00 (roof) φ = 0,80 (stories with correlated occupancies)

Table 3 FUSEIS beam sections

Floor No	IPE			SHS			CHS		
	0,16g	0,24g	0,36g	0,16g	0,24g	0,36g	0,16g	0,24g	0,36g
1	330	330	400	280×8	280×8	300×10	355,6 ×8	355,6×8	355,6×10
2	300	300	330	240×8	240×8	260×8	273,0×10	273,0×10	323,9×8
3	270	270	300	200×8	200×8	240×8	244,5×8	244,5×8	273,0×10
4	220	220	270	160×8	160×8	200×8	193,7×8	193,7×8	244,5×8
5	160	160	180	100×8	100×8	140×6	139,7×6	139,7×6	168,3×6

Table 4 FUSEIS columns' sections

No 1	0,16g - 0,24g	RHS 300×200×20
No 2	0,36g	RHS 400×300×20

Table 5 Modal periods and participating masses

FUSEIS	Ground Acceleration	Mode	T(s)	Participating mass ratios (%)	Sum of Masses (%)
IPE	0,16g -0,24g	1	1,354	77,6	92,4
		2	0,459	14,8	
	0,36g	1	1,147	75,1	90,9
		2	0,368	15,8	
SHS	0,16g -0,24g	1	1,373	76,2	91,2
		2	0,477	15,0	
	0,36g	1	1,162	74,8	90,6
		2	0,379	15,8	
CHS	0,16g -0,24g	1	1,355	75,7	90,8
		2	0,466	15,1	
	0,36g	1	1,156	75,0	91,0
		2	0,377	16,0	

Table 6 Fuseis – Ωvalues

IPE						SHS						CHS					
0,16		0,24		0,36		0,16		0,24		0,36		0,16		0,24		0,36	
$\frac{1}{\Omega}$	$\frac{\max\Omega}{\min\Omega}$	$\frac{1}{\Omega}$	$\frac{\max\Omega}{\min\Omega}$	$\frac{1}{\Omega}$	$\frac{\max\Omega}{\min\Omega}$	$\frac{1}{\Omega}$	$\frac{\max\Omega}{\min\Omega}$	$\frac{1}{\Omega}$	$\frac{\max\Omega}{\min\Omega}$	$\frac{1}{\Omega}$	$\frac{\max\Omega}{\min\Omega}$	$\frac{1}{\Omega}$	$\frac{\max\Omega}{\min\Omega}$	$\frac{1}{\Omega}$	$\frac{\max\Omega}{\min\Omega}$	$\frac{1}{\Omega}$	$\frac{\max\Omega}{\min\Omega}$
0,39		0,56		0,57		0,37		0,52		0,56		0,38		0,54		0,56	
0,40		0,59		0,71		0,36		0,53		0,65		0,38		0,55		0,68	
0,40	1,19	0,59	1,23	0,70	1,23	0,37	1,15	0,54	1,16	0,64	1,17	0,38	1,12	0,55	1,13	0,66	1,21
0,46		0,67		0,70		0,41		0,59		0,64		0,42		0,61		0,66	
0,43		0,61		0,69		0,36		0,51		0,59		0,42		0,60		0,60	

composite beams and the columns, rotational springs were assigned at the composite beams' ends. The spring constants were calculated analytically for each frame according to CEN (2004) EC3 and CEN (2005) EC4 taking into account the longitudinal reinforcement of the concrete flange.

Vertical loading was equal for all stories and masses were lumped at the joints. Steel grade of

the non-dissipative structural members was S355 and for the dissipative elements (the fuses) S235 to eliminate the risk of possible overstrength of the dissipative elements. Design data for the frames are summarized in Table 2. A preliminary value of the behavior factor q = 5 was employed that is discussed later.

The described layout was followed for all nine frames. All frames were designed according to the provisions of EC3 for ULS and SLS. Limitations on 2nd order effects according to EC8 were also taken into account. In all cases the value of the interstory drift sensitivity coefficient θ was between 0,1 and 0,2 indicating that a frame with FUSEIS system is flexible. The relevant seismic action effects were then multiplied by a magnification factor 1/(1 - θ). Interstory drifts were limited to 0,0075 (buildings having ductile non-structural elements) - EC 8. Drift considerations lead to the determination of the FUSEIS sections through a number of iterations on a variety of section sizes.

Design was based on multi modal response spectrum analysis using a linear-elastic model of the structure and a design spectrum. The analysis showed that the first mode of vibration (Fig. 6a) activated approximately 75% of the mass while few more modes were needed to reach 90% as required by Codes (Table 5). Table 3 and Table 4 summarize the system fuses used and the system columns.

The dissipative zones are restricted within the RBS sections of the FUSEIS beams so that the overall stability of the structure was not substantially affected by their hysteretic behavior. Generally the full plastic moments of the RBS sections develop with no reduction due to the presence of high shear and compression forces since they fulfill the following conditions

(1) Axial forces

$$\frac{N_{Ed,M}}{N_{pl,Rd}} \leq 0,15 \tag{6}$$

(2) Shear resistance

$$\frac{V_{CD,Ed}}{V_{b,pl,Rd}} \leq 1 \tag{7}$$

(3) Moment capacity (critical check)

$$\frac{M_{Ed}}{M_{pl,RBS,Rd}} = \frac{1}{\Omega} \leq 1,0 \tag{8}$$

where $V_{CD,Ed} = \frac{2 \cdot M_{pl,RBS,Rd}}{l_{RBS}}$ is the capacity design shear force due to application of moments of resistance $M_{pl,RBS,Rd}$ of the RBS sections in opposite direction and l_{RBS} is the length of the reduced section.

To achieve a global dissipative behavior of the structure, it was checked that the ratios Ω do not differ from the minimum value Ω by more than 25%. The following Table 6 summarizes the Ω values for the examined frames.

At global inter-story drift rotations, $\theta_{gl,}$ of the frame during seismic loading the dissipative elements, the beams, exhibit larger plastic rotations calculated from the following equation where θ_{gl} was limited to the drift at the CPLS

$$\theta_{pl,RBS} = \frac{L}{l_{RBS}} \theta_{gl} \tag{9}$$

The non-dissipative elements, the FUSEIS beams-to-columns connections and the system

columns, were designed for increased values of internal forces and moments compared to those derived from analysis taking into account the section overstrength Ω and the material overstrength factor γ_{ov}=1,25 in accordance with the provisions of EC8 as follows

$$N_{Rd}(M_{Ed}, V_{Ed}) \geq N_{Ed,G} + 1{,}10\gamma_{ov} \cdot \Omega \cdot N_{Ed,E} \quad (10)$$

Lateral torsional buckling verifications for the FUSEIS beams are generally not necessary due to their small length.

5. Non- linear static analysis (pushover) and evaluation of the behavior factor q

The structural models used for elastic analysis were extended to include the response of structural elements beyond the elastic state via a non-linear static analysis (pushover). The principal objective of this investigation was to estimate the behavior factor q.

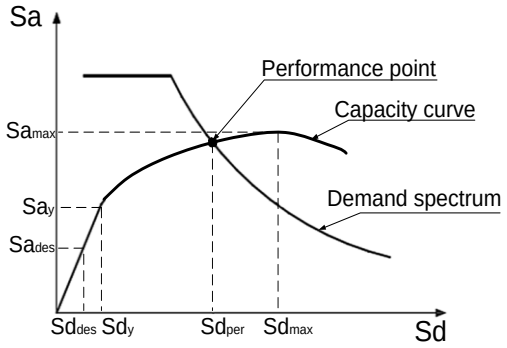

Fig. 4 Definition of the performance point

Hinge Properties (α_{pl} =shape factor)						
	IPE		SHS		CHS	
Point	$M/M_{pl,RBS}$	$\theta/\theta_{pl,RBS}$	$M/M_{pl,RBS}$	$\theta/\theta_{pl,RBS}$	$M/M_{pl,RBS}$	$\theta/\theta_{pl,RBS}$
E-	-0,6	-45	-0,4	-30	-0,2	-30
D-	-0,6	-40	-0,4	-25	-0,2	-25
C-	$-\alpha_{pl}$	-40	$-\alpha_{pl}$	-25	$-\alpha_{pl}$	-25
B-	1	0	-0,6	0	-1	0
A	0	0	0	0	0	0
B	1	0	0,6	0	1	0
C	α_{pl}	40	α_{pl}	25	α_{pl}	25
D	0,6	40	0,4	25	0,2	25
E	0,6	45	0,4	30	0,2	30

Acceptance Criteria ($\theta/\theta_{pl,RBS}$)			
	IPE	SHS	CHS
IO	15	5	6
LS	20	12	10
CP	35	18	16

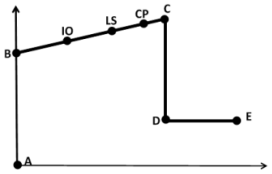

Fig. 5 Non-linear hinge parameters for IPE,SHS &CHS

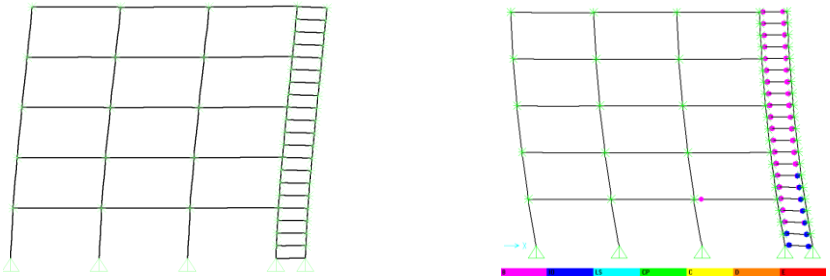

(a) (b)

Fig. 6 Deformed frame with SHS fuses (a) at fundamental mode and (b) at the performance point

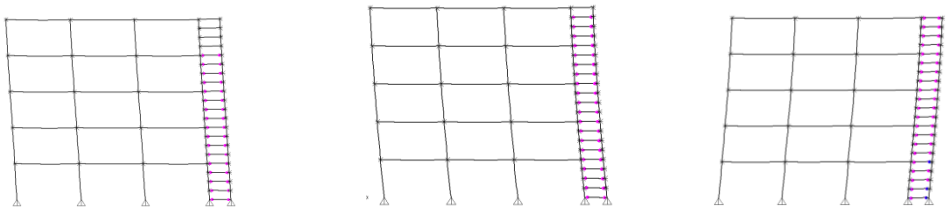

SHS PGA = 0.16g SHS PGA = 0.24g SHS PGA = 0.36g

Fig. 7 Hinges at the performance Point

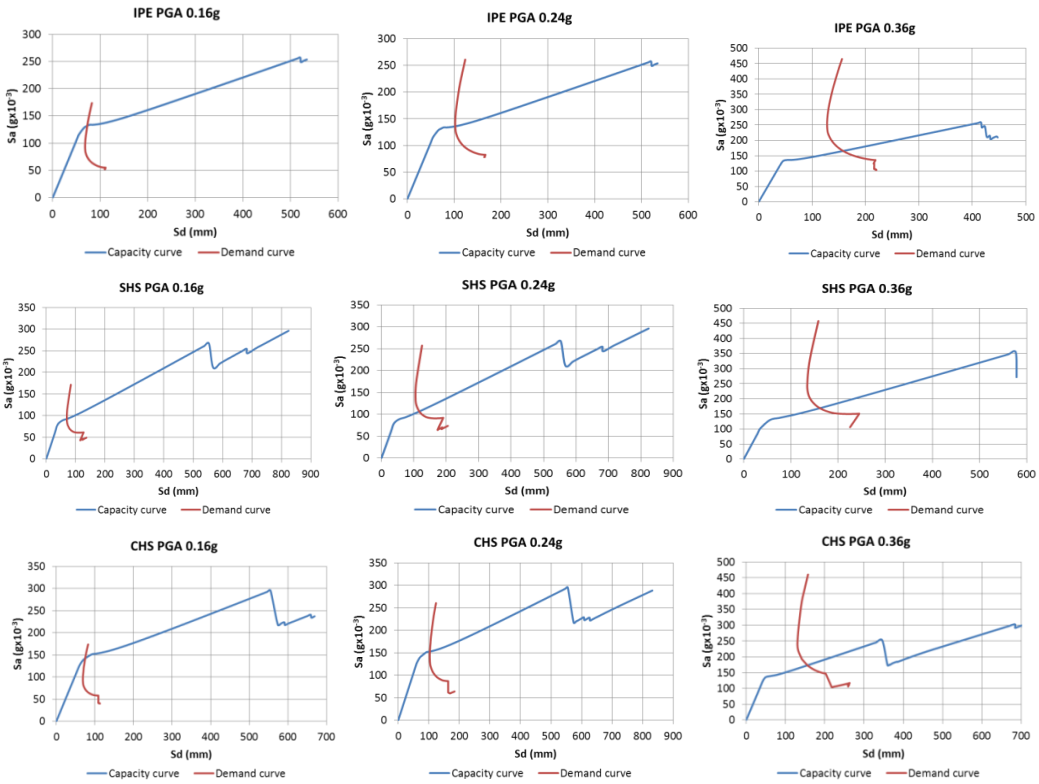

Fig. 8 Evaluation of performance point

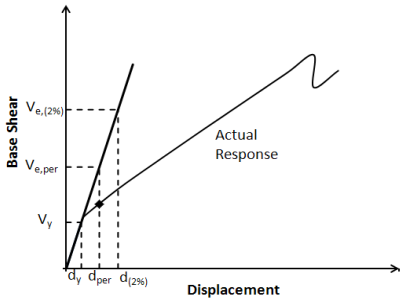

Fig. 9 Typical pushover response curve for evaluation of behavior factors

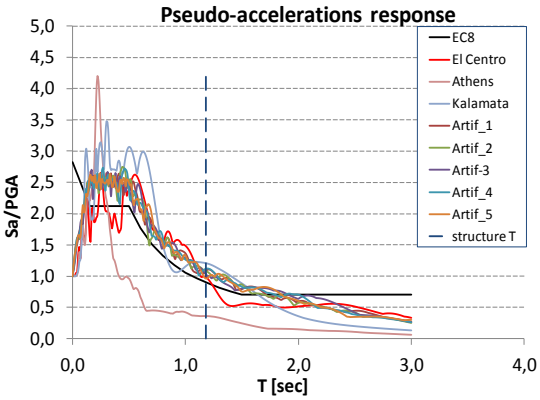

Fig. 10 Acceleration spectra of the examined records and design Code spectrum

Table 7 Behavior factor calculation

FUSEIS BEAMS	0,16g			0,24g			0,36g		
	q_μ	Ω	q	q_μ	Ω	q	q_μ	Ω	q
IPE	3,31	2,99	9,91	3,31	1,97	6,51	3,81	1,26	4,79
SHS	3,97	2,26	8,99	3,97	1,51	6,01	5,79	1,09	6,31

Table 8 Experimental – analytical drifts

	IPE				SHS				CHS			
	Exp.	Analytical			Exp.	Analytical			Exp.	Analytical		
		0,16g	0,24g	0,36g		0,16g	0,24g	0,36g		0,16g	0,24g	0,36g
SLS	0,80	0,39	0,55	0,52	1,00	0,44	0,57	0,66	1,00	0,50	0,55	0,54
ULS	2,50	0,61	0,85	1,84	2,40	0,67	1,25	1,53	2,15	0,76	0,93	1,96
CPLS	3,90	0,85	2,00	3,51	4,70	1,25	2,65	3,02	5,20	0,88	1,59	3,32

The analysis was carried out under conditions of constant gravity loads $1,0 \cdot G + 0,3 \cdot \varphi \cdot Q$ and monotonically increasing lateral loads. Two vertical distributions of the lateral loads were applied: a "uniform" pattern and a "modal" pattern distribution in the direction under consideration. The results of the analysis according to the fundamental mode of vibration, 1st mode, are presented

hereafter. The analysis was based on the assumption that the mode shape remains unchanged after the structure yields. P–Delta effects were also taken into account.
In pushover analysis the behavior of the structure is characterized by a capacity curve that represents the relationship between base shear force and top displacement and the demand curve for the design earthquake which was based on ATC-40 (1996). The performance point is defined as the intersection of the demand curve with the capacity curve (Fig. 4).

In the implementation of pushover analysis accurate modeling of the hinges is crucial. The model requires the determination of the nonlinear properties of each component in the structure that are quantified by strength and deformation capacities. Non-linear hinge elements were assigned to the structural members. The fuses hinges were inserted at the ends of the reduced parts and their properties were derived from the calibrated models of the tests (Fig. 5).

At the start of the calculations potential plastic hinges were also inserted at the ends of the composite beams, the columns and the system columns to check if they also behave inelastic during the seismic event. For these elements the hinge properties were determined according to FEMA-356 (2000) documents. Specifically, for the composite beam the plastic moment, considered for the definition of the plastic hinges, derived from the plastic modulus of the steel section disregarding the participation of the longitudinal reinforcement. This assumption had a minor effect on the results, however in a more detailed design the longitudinal reinforcement should be taken into account. The non-linear moment-curvature relationships were determined by neglecting the axial forces of the floor beams due to the composite slab diaphragm and considering axial forces in the columns as equal to those resulting from gravity loads in the seismic combination. Fig. 6b shows the deformed frame with SHS fuses at the performance point; it is obvious that plastic hinges formed only in the reduced parts of the fuses. In subsequent analyses potential hinges were introduced only in the fuses.

The distribution of plastic hinges is given indicatively for the building frames with SHS sections in Fig. 7 and the evaluation of the performance point for all the examined building frames is given in Fig. 8.

As expected the weak beam strong column concept was fulfilled for all frames studied and the sequence of plastic hinges at beams' ends started from lower to top stories.

Besides the assessment of the structural performance of the building frames, pushover analysis also offered the possibility to estimate their behavior factor. Due to the flexibility of the system $T_1 \geq T_c$ the 'equal displacement rule' was applied. Fig. 9 shows the typical pushover response curve for the evaluation of behavior factors.

The behavior factor, q, accounts for the inherent ductility and overstrength of a structure. It may be generally expressed in the following form taking into account the above two components

$$q = q_{\mu} \cdot \Omega \tag{11}$$

The structure ductility, q_{μ}, is defined in terms of the Elastic Base Reaction that corresponds to 2% drift (V_e) to the Idealised Yield Strength - First hinge (V_y) (Fig. 9), as following

$$q_{\mu} = \frac{V_e}{V_y} \tag{12}$$

The ID equal to 2% was determined experimentally and corresponds to the maximum force reached.

The structural overstrength is defined as the ratio of the Idealised Yield Strength - First hinge V_y to the Design Strength (V_d), as following

$$\Omega = \frac{V_y}{V_d} \tag{13}$$

The Design Strength (V_d) was based on the fundamental vibration mode which had the largest participation to the vibrating mass and was determined from $V_d = \eta \cdot M \cdot S_d(T)$, where n is the modal participating mass ratio, M is the total mass and $S_d(T)$ is the spectral acceleration that derives from the design spectra for the fundamental mode.

The system's behavior is characterized by high values of ductility whereas its overstrength is dependent on the intensity of the design earthquake. The calculated q factors are summarized in Table 7. All q values are above 5, the value that was considered for the initial design. It is recommended to adopt q = 5 for a FUSEIS system, since higher values, although possible, would result in a more flexible frame and lead to increased θ and drift values.

The seismic behavior was also evaluated for the different ground motion intensities (0,16g, 0,24g, 0,36g), for three performance levels (Limit states): SLS where the ground earthquake motion was reduced to 0,5 (EC8-1 §4.4.3), ULS where the intensity of the earthquake action was equal to the design one and CPLS where the ground earthquake motion was increased to 1,5. Specifically, the drift of the SLS was compared to the experimental drift at yield, the drift of the ULS was compared to the experimental drift when the max force was reached and the drift of CPLS was compared to the experimental max drift. The comparison for each type of section is shown in Table 8. The calculated drifts were in all cases lower than the corresponding experimental drifts. It should be noted that the experimental drift values are similar to the values given by FEMA-356 (2000) for the Steel Moment Frames (SLS equal to 0,70, ULS equal to 2,50, CPLS equal to 5,00).

It was observed that at the CPLS performance point the hinges formed in the fuses were at the Immediate Occupancy level which means that the structure has light to moderate overall damages with minor local yielding of the fuses.

6. Non- linear dynamic analysis (time-history)

In order to define time-dependent response of steel buildings with FUSEIS1-1 when designed according to the provisions of the European Codes under real earthquake conditions, non - linear dynamic analyses on a representative 2D building frame were performed. Such analyses allow the determination of the behavior of a building frame over a wide range of events. Recent Greek earthquakes that caused severe damage and loss of human lives as well as the El Centro earthquake widely used as reference were selected. Additionally, artificial records were examined. The relevant information is given in Table 9. The Records were scaled adequately to comply with the seismic zone 0,36g. Fig. 10 gives the acceleration spectra of the selected records together with the design spectrum and the fundamental period of the frame.

For composite beam to column connections two cases were examined, one with partially fixed composite beams (MRF) by means of appropriate rotational springs and one with hinged connections. The plastic hinges assigned at the ends of the composite beams were adjusted to fit the end releases. Indicatively, the analyses conducted for the building frame with the SHS FUSEIS beams are presented hereafter. In all cases examined the behavior of the frame was similar and verified the pushover analysis. The sequence of plastic hinges started at beams' ends from lower stories up to upper stories contributing to the energy dissipation of the building frame.

The response of the frame under the above mentioned ground excitations was evaluated in terms of displacement histories. Fig. 11 displays roof displacements versus time for all the examined ground motions for both cases studied, partially fixed and hinged composite beams.

It may be seen that when the FUSEIS system is combined with moment resisting frame (MRF) action, the building returns close to its initial position with negligible residual displacements at the end of the event. This is due to the fact that inelastic deformations concentrate in the FUSEIS system while the moment resisting frame remains elastic and drives the structure to return to its initial state. On the contrary, when the composite beams are hinged, even though the plastic hinges are also formed in the FUSEIS, the structure is not able to return explaining thus the residual displacements.

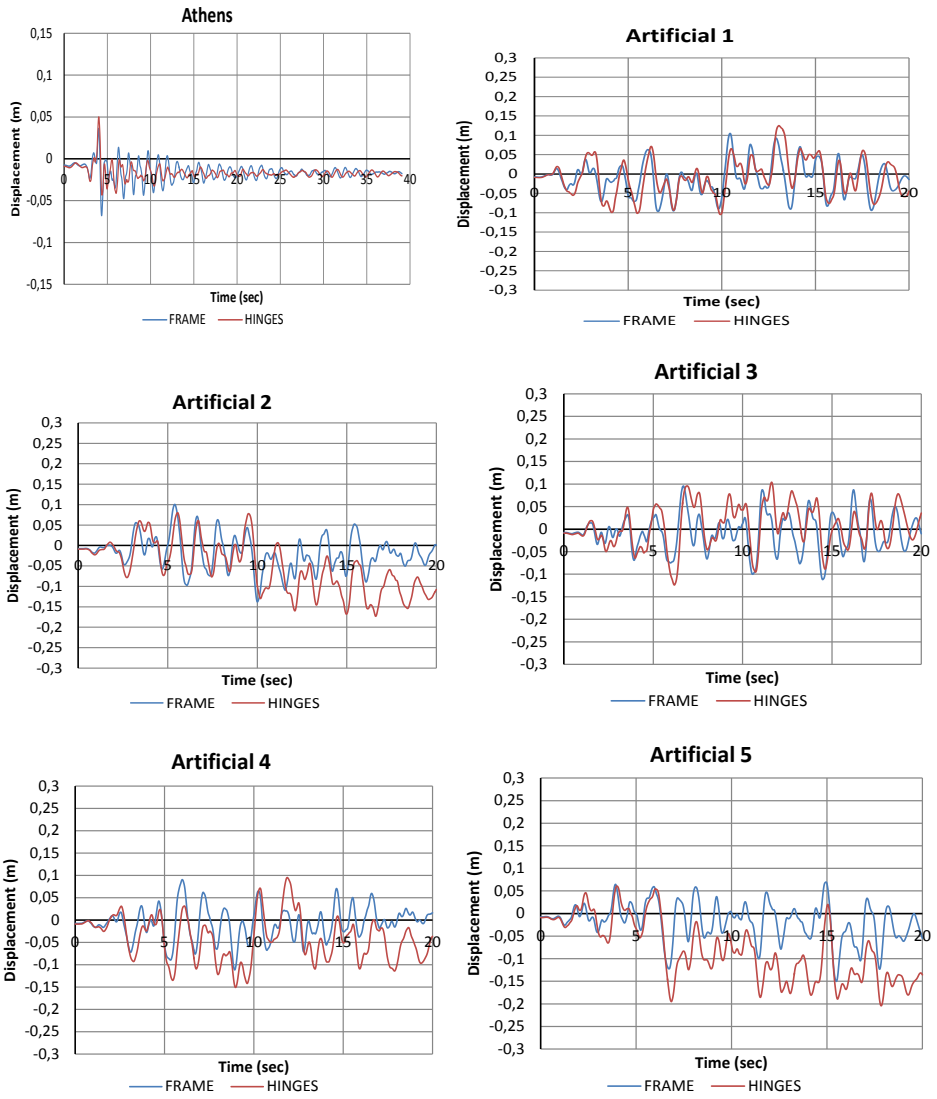

Fig. 11 Displacement responses for all the examined ground motions

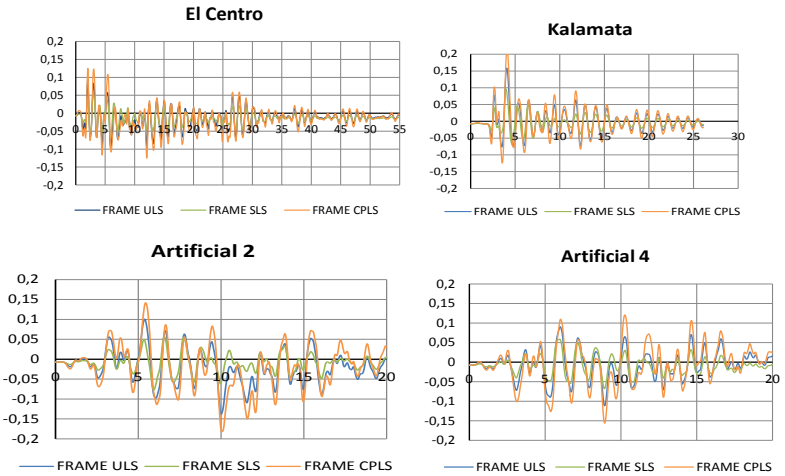

Fig. 12 Displacement responses for the SLS, ULS and CPLS limit states

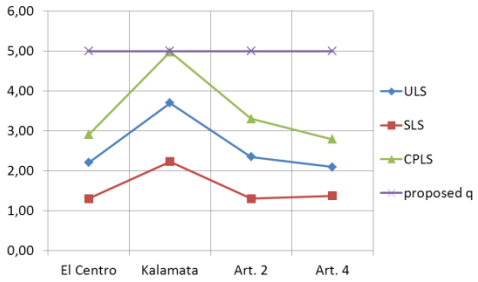

Fig. 13 Demanded vs proposed behavior factor

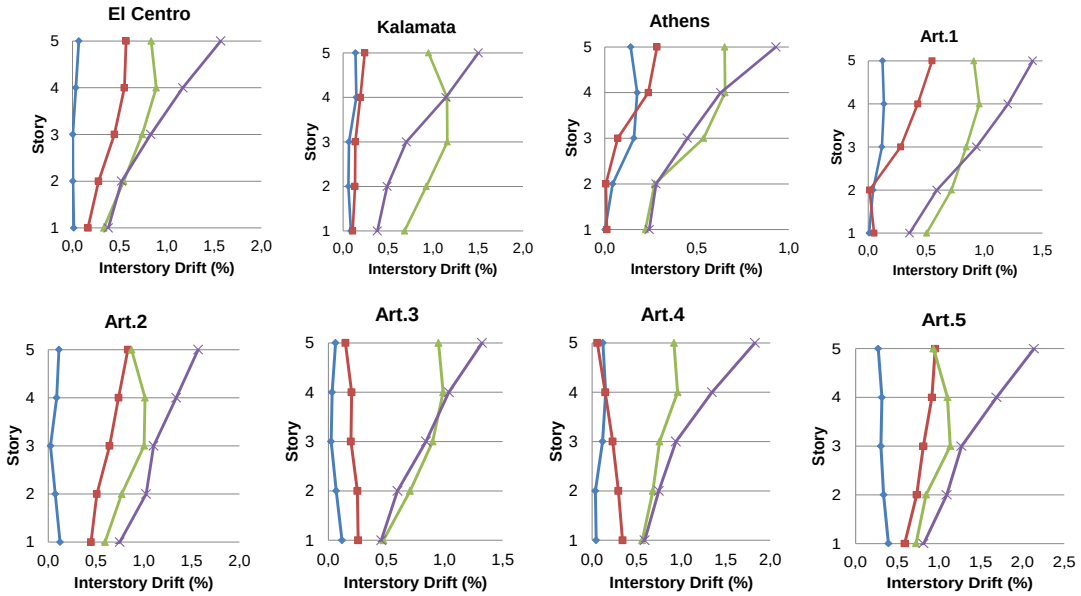

Fig. 14Maximum – residual Interstory drifts for the examined earthquakes

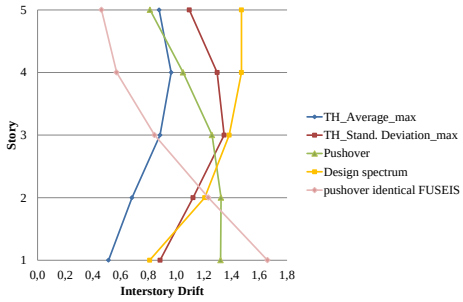

Fig. 15 Interstory drift comparison for linear, pushover and time history analyses

Table 3 Types and configurations of the seismic records

Type	Location	PGA[g]
Near field European	Kalamata (1985)	0,294
	Athens (1999)	0,298
Near field International	El. Centro	0,355
Artificial accelerograms 1-5	-	0,300

Table 10 Residual Drifts

Earthquakes	Residual driftframe (%)	Residual drifthinges (%)
ElCentro	0,030	0,400
Athens	0,104	0,200
Kalamata	0,076	0,160
Artificial 1	0,085	0,259
Artificial 2	0,004	0,633
Artificial 3	0,060	0,210
Artificial 4	0,095	0,215
Artificial 5	0,323	0,798

Table 11 Behavior factors for various performance levels

Seismicrecords		SLS	ULS	CPLS
ElCentro	d_{max}	0,056	0,095	0,125
	q	1,30	2,21	2,91
Athens	d_{max}	-	0,036	-
	q	-	0,84	-
Kalamata	d_{max}	0,096	0,159	0,214
	q	2,23	3,70	4,98
Art. 1	d_{max}	-	0,105	-
	q	-	2,44	-
Art. 2	d_{max}	0,056	0,101	0,142
	q	1,30	2,35	3,30
Art. 3	d_{max}	-	0,096	-
	q	-	2,23	-
Art. 4	d_{max}	0,059	0,09	0,120
	q	1,37	2,09	2,79
Art. 5	d_{max}	-	0,07	-

Table 12 Comparison of maximum interstory- drifts

Earthquakes	MaxInt. driftframe (%)	MaxInt.drifthinges (%)	Ratio
ElCentro	0,89	1,57	1,76
Athens	0,65	0,93	1,43
Kalamata	1,16	1,5	1,29
Artificial 1	0,96	1,42	1,48
Artificial 2	1,01	1,57	1,55
Artificial 3	0,99	1,32	1,33
Artificial 4	0,96	1,83	1,91
Artificial 5	1,13	2,14	1,89

After a seismic event, if no failure is observed, residual story drift may constitute a significant criterion for the evaluation of the building. The residual drifts, obtained by dividing the residual displacements at the top by the frame height, are summarized in Table 10. It may be seen that residual drifts in the first case are limited to a maximal value of 0,323%and in the second case to 0,798%. FEMA 356 allows for steel MRF's 1% residual drifts at life safety structural performance. The very low values of the residual drifts, with one exception, for combinations of FUSEIS system with MRF's allows the statement that such systems could be regarded as self-centering.

The behavior of the MRF frame with FUSEIS 1-1 was also evaluated for thethree performance levels SLS, ULS and CPLS. This was done by further scaling the already scaled to PGA = 0,36gground motions with the scaling factors 0,5, 1,0 and 1,5. Results for the El Centro, Kalamata, Artificial 2 and 4 earthquakes are shown in Fig. 12. The residual drifts for the CPLS limit state were higher than for the other limit states as expected, but in all cases lower than the limit value 1% maintaining the advantages of self- centering systems.

The behavior factor for the system was obtained from equation

$$q = \frac{d_{max}}{d_{el}} \tag{14}$$

where d_{max} is the maximum displacement (or ultimate displacement) that the system sustained during the examined earthquakes and d_{el}= 0,043m was the maximum displacement as determined by a linear analysis based on the design response spectrum. The behavior factor demands for various performance levels are given in the following Table 11. Fig. 13 shows the comparison of the demands for behavior factors to the proposed design value.

Comparing the maximum interstory drift for the two cases (partially fixed and hinged composite beams) it was found that the drift values for the MRF are lower than the values for the hinged frame (Fig. 14). The maximum inter-story drifts and the residual drifts are given in Fig. 14 and Table 12. For the MRF system the maximum drifts are close to the limit value of SLS (1%) whereas the maximum drifts in the case of the hinged frames are at the ULS (<2,4%). Moreover, the self-centering behavior of the MRF is confirmed since the residual drift values are close to 0.

7. Comparison of the results

Linear, pushover and time history analyses enabled the determination of the contributions of FUSEIS beams and MRF to the total response of a building and provided the basic guidelines for the design. Besides the results of the individual analyses given in detail in sections 4-6 their

validity was also verified through a comparison of the interstory drifts, that was considered to be the most representative parameter for the behavior of a building (Fig. 15).

For the time history analysis two curves are given. The blue represents the mean values and the red 95% fractile values of maximum drifts. The diagram shows that the time history curves are similar to the design spectrum curve and the interstory drift increases from the lower to the upper stories. The pushover curve is more unfavourable since a soft story plastic mechanism is formed at the ground level.

An additional analysis was carried out using identical FUSEIS sections SHS 300x300x10 in all floors which gave large interstory drift deviation (0,4-1,7%) and as a result less uniform response.

8. Conclusions

The above study illustrates the successful application of the innovative FUSEIS 1-1 system. The following observations are worth noting:

The system resists lateral loads as a vertical Vierendeel beam.

Inelastic deformations are strictly limited to the dissipative elements preventing the spreading of damage into the rest of the structural members (slab, beams, columns). The devices and the frames with the devices have a very good behavior: strong, stiff, large capacity of energy absorption.

The structural system may be designed as more flexible/rigid depending on the section types and their distribution between floor levels. The number of stories and supporting weight strongly affects the required sections and geometry. The seismic resistance of a building may be obtained by appropriate provision of a number of FUSEIS systems in the relevant directions.

The innovative system provides an architecturally versatile solution for the lateral stability of building structures compared to braced frames as the fuses can be positioned in small areas of the building and do not interrupt the architectural plan. The fuse elements can also constitute visible parts of the building indicating its seismic resistant system.

Sequential plasticization may be allowed by appropriate selection of the sections of the dissipative elements.

The dissipative elements are easily replaceable if they are damaged after a strong seismic event; they are small and are not part of the gravity loading resistant system. Assembling and disassembling is easy from a practical point of view.

The FUSEIS1-1 system is able to guarantee an efficient control both on drift and displacement deformations, exhibiting a self-centering behavior.

The proposed q-factor for buildings with FUSEIS1-1 is 5.

The seismic design of frames with dissipative FUSEIS as described in Section 4 conforms to the verifications of Eurocode 8 with some rearranged clauses. These modifications and additional rules are included in the relevant Design Guide (Vayas *et al.*, 2012).

Acknowledgments

The research presented is made in the framework of the European Research Project RFSR-CT-2008-00032: “Dissipative devices for seismic resistant steel frames (Fuseis)”. The financial

contribution of the Research Fund for Coal and Steel of the European Community is gratefully acknowledged.

References

ATC – 40 (1996), Seismic evaluation and retrofit of concrete buildings, Applied Technology Council, California.

CEN (2003), "European standard EN1993-1-1: Eurocode 3: Design of steel structures. Part 1-1: General rules and rules for buildings", Comité European de Normalisation, Brussels.

CEN (2004), "European standard EN 1993-1-8: Eurocode 3: Design of steel structures. Part 1-8: Design of joints", Comité European de Normalisation, Brussels.

CEN (2005), "European standard EN1994-1-1: Eurocode 4: Design of composite steel and concrete structures. Part 1-1: General rules and rules for buildings", Comité European de Normalisation, Brussels.

CEN (2003), "European standard EN1998-1-1: Eurocode 8: Design of structures for earthquake resistance. Part 1-1: General rules, seismic actions and rules for buildings", Comité European de Normalisation, Brussels.

Christopoulos, C., Filiatrault, A., Folz, B. and Uang, C.M (2002), "Post-Tensioned Energy Dissipating Connections for Moment-Resisting Steel Frames", *ASCE J. Struct. Eng.*, **128**(9), 1111-1120.

Dargush, G. and Soong, T. (1995), "Behavior of metallic plate dampers in seismic passive energy dissipation systems", *Earthq. Spec.*, **11**(4), 545-568.

Dimakogianni, D., Dougka, G. and Vayas, I. (2012), "Innovative seismic-resistant steel frames (FUSEIS 1-2) experimental analysis", *Steel Construct. Des. Res.*, **5**(4), 212-221.

FEMA – 356 (2000), Prestandard and Commentary for the seismic rehabilitation of Buildings, Washington.

FEMA – P695 (2009), Quantification of building seismic performance factors, Washington.

Herning, G., Garlock, M. and Vanmarcke, E. (2009), "Evaluation of design procedure for steel self-centering moment frames", *Proceedings of Steel Structures in Seismic Areas (STESSA)*, Philadelphia PA, U.S.A., August.

Karydakis, P.H. (2011), "Innovative systems for stiffness and energy dissipation, INSTED", Ph.D. Dissertation, National Technical University of Athens, Athens.

Nakashima, M. (1995), "Strain-hardening behavior of shear panels made of low-yield steel. i:test.", *J. Struct. Eng.*, **121**(12), 1742-1749.

Nakashima, M., Akazawa, T. and Tsuji, B. (1995), "Strain-hardening behavior of shear panels made of low-yield steel.ii:model", *J. Struct. Eng.*, **121**(12), 1750-1757.

Maheri, M. R. and Akbari, R. (2002), "Seismic behaviour factor, R, for steel X-braced and knee-braced RC buildings", *Eng. Struct.*, **25**(12), 1505-1513.

Plumier, A., Doneux, C., Castiglioni, C., Brescianini, J., Crespi, A., Dell'Anna, S., Lazzarotto, L., Calado, L., Ferreira, J., Feligioni, S., Bursi, O., Ferrario, F., Sommavilla, M., Vayas, I., Thanopoulos, P. and Demarco, T. (2004), *Two IN Novations for Earthquake Resistant Design - The INERD Project, Final Report*, Research Programme of the Research Fund for Coal and Steel.

SAP (2000), Csi Computers and Structures Inc., www.csiberkeley.com

Sabelli, R., Mahin, S. and Chang, C. (2003), "Seismic demands on steel braced buildings with buckling-restrained braces", *Eng. Struct.*, **25**(5), 665-666.

Saeki, E., Iwamatu, K. and Wada, A. (1996),"Analytical study by finite element method and comparison with experiment results concerning buckling-restrained unbonded braces", *J. Struct. Construct. Eng.*, Architectural Institute of Japan, 484, 111- 120.

Tena-Colunga, A. (1997), "Mathematica modeling of the ADAS energy dissipation device", *Eng. Struct.*, **19**(10), 811-820.

Tsai, K.C., Chen, H.W. and Hong, C. and Su, Y. (1993), "Design of steel triangular plate energy absorbers for seismic-resistant construction", *Earthq. Spec.*, **9**(3), 505-528.

Vayas, I., Karydakis, P.H., Dimakogianni, D., Dougka, G., Castiglioni, C.A. and Kanyilmaz, A. (2012), "Dissipative devices for seismic resistant steel frames - The FUSEIS project, design guide", Research Programme of the Research Fund for Coal and Steel.

Vayas, I., Karydakis, P.H., Dimakogianni, D., Dougka, G., Castiglioni, C.A. and Kanyilmaz, A. (2013), "Dissipative devices for seismic-resistant steel frames (fuseis)", Research Fund for Coal and Steel, European Commission, EU 25901 EN, 2013.

Vayas, I. and Thanopoulos, P. (2005), "Innovative dissipative (INERD) pin connections for seismic resistant braced frames", *Int. J. Steel Struct.*, **5**(5), 453-464.

Vayas, I. and Thanopoulos, P. (2006), Dissipative (INERD) "Verbindungenfür stahltragwerke in erdbebengebieten", *Stahlbau*, **75**(12), 993-1003.

Vayas, I., Thanopoulos, P. and Castiglioni C. (2007), "Stabilitätsverhalten von Stahlgeschossbautenmitdissipativen INERD unter Erdbebenbeanspruchung", *Bauingenieur*, **82**(3), 125-133.

CC